



HAL
open science

Design and experimental validation of a voltage sensing-current cancellation Common Mode linear active filter

B. Mohamed Nassurdine, Pierre-Etienne Lévy, D Labrousse, J. L. Schanen, X. Maynard, S. Carcouet

► **To cite this version:**

B. Mohamed Nassurdine, Pierre-Etienne Lévy, D Labrousse, J. L. Schanen, X. Maynard, et al.. Design and experimental validation of a voltage sensing-current cancellation Common Mode linear active filter. 2022 24th European Conference on Power Electronics and Applications (EPE'22 ECCE Europe), Sep 2022, Hannover, Germany. <hal-03779387>

HAL Id: hal-03779387

<https://hal.science/hal-03779387v1>

Submitted on 16 Sep 2022

HAL is a multi-disciplinary open access archive for the deposit and dissemination of scientific research documents, whether they are published or not. The documents may come from teaching and research institutions in France or abroad, or from public or private research centers.

L'archive ouverte pluridisciplinaire **HAL**, est destinée au dépôt et à la diffusion de documents scientifiques de niveau recherche, publiés ou non, émanant des établissements d'enseignement et de recherche français ou étrangers, des laboratoires publics ou privés.



HAL Authorization

Design and experimental validation of a Voltage Sensing-Current Cancellation Common Mode Linear Active Filter

B.Mohamed Nassurdine^{1,3,4}, PE.Lévy¹, D.Labrousse², JL.Schanen³, X.Maynard⁴, S.Carcouet⁵

¹ Univ. Paris-Saclay, ENS-Paris Saclay, SATIE, F-91190 Gif-sur-Yvette, France

² Le Cnam, SATIE, UMR 8029, F-75003 Paris, France, HESAM Université

³ Univ. Grenoble Alpes, CNRS, Grenoble INP, G2Elab, F-38000 Grenoble, France

⁴ CEA-Liten, F-38000 Grenoble, France

⁵ CEA-Leti, F-38000 Grenoble, France

E-Mail : bacar.mohamed_nassurdine@ens-paris-saclay.fr, pierre-etienne.levy@ens-paris-saclay.fr, denis.labrousse@satie.ens-cachan.fr, jean-luc.schanen@grenoble-inp.fr, xavier.maynard@cea.fr, sebastien.carcouet@cea.fr

Keywords

«DC-DC converter», «Electromagnetic Interference (EMI) », «Active filter», «Boost», «Switched-mode power supply»

Abstract

In recent years, the study and design of linear active EMI filters (AEF) have been the subject of many research papers. Different modeling approaches to study the performances of the AEF have been proposed. The aim of this paper is to introduce a methodology to design a Common Mode (CM) AEF able to cancel the CM electromagnetic interference noise in a given frequency range. The active filter is analyzed based on the CM noise model of a boost converter. The first part of the study is devoted to the modeling of the electrical structure of the filter and the definition of component values. In this part, attenuation, design rules and stability of AEF are addressed in detail. The second part of the study is dedicated to the simulations and experiments to validate the proposed methodology. This step allows realizing a functional prototype that complies with the DO160 standard (aeronautics) up to 1 MHz

I. Introduction

Nowadays, our daily life can no more be dissociated from the use of Switched-Mode Power Supply (consumer electronics, transportation ...). These converters are sources of electromagnetic interferences (conducted and radiated) due to the high gradients of voltages and currents [1], [2]. With the coexistence of various electronic apparatus within the same system, Electromagnetic Compatibility (EMC) has become a major issue for manufacturers and users.

Usually, EMC conformity including aeronautic conformity (DO160 standard) in the 'RF' (Radio Frequency) range (150 kHz – 30 MHz) can be met using passive filters, for differential-mode (DM) and common-mode (CM) noise. However, passive filters are quite expensive and bulky, and may represent up to 30% of the cost, weight, and volume of a power converter. Therefore, hybrid filtering (active plus passive) appears to be a promising alternative to reduce the size, weight, and cost of converters. A volume reduction greater than 40% has been reported in [3],[4]. In hybrid filtering, low frequency interferences are filtered by AEF and high frequency interferences by passive filter. The principle of AEF consists of detecting an output quantity (voltage or current) at the converter's input and comparing it to a zero reference (ground). The error is processed in an analog- (Op amp) or digital- (DSP or FPGA) way to obtain the necessary gain to reject noises. In the literature, two main structures of AEF have been reported: the feedback and the feedforward topologies. A comparative analysis of these two topologies was made in [5] and it was concluded that the feedback topologies is more easily controllable than the feedforward. Indeed, for efficient filtering, the feedforward gain must be equal to one [3], [5]: this condition is hard to achieve due to the non-linearity and parasitic elements of the passive components

used for the detection and injection in the AEF. On the other hand, four feedback topologies are available depending on the sensing and the cancelling methods.

Noise sensing topologies involve noise current and noise voltage sensing. Current sensing uses a very high bandwidth current transformer, which can become bulky and can also saturate depending on noise level, contrary to voltage sensing, which requires only RC circuit. The current sensing however has the interest of galvanic isolation. Noise injection techniques can use either current or voltage injection. In current cancellation, the active circuit drives a voltage across an injection capacitor resulting in cancellation current injected in the circuit. In voltage cancellation, the active circuit drives a voltage injection transformer that injects the cancellation voltage in the main circuit. Some of the commonly used noise sensing and noise injecting topologies are given in [6] and shown in Fig.1. In this figure, the CM noise generation of the converter is represented using a Norton equivalent circuit. An experimental study in [6] shown that current injection topologies provide better attenuation than voltage injection for CM noise filtering. On the other hand, voltage injection attenuates more than current injection topologies for DM noise filtering. An analytical study validates these results.

As current injection topologies provide better attenuation than voltage injection for common mode filtering and taking into account its simplicity and lightness, a voltage sensing-current cancellation common mode topology (VSCC) has been chosen and studied in this paper for a boost power converter (14V/42V - 115 kHz – 27W).

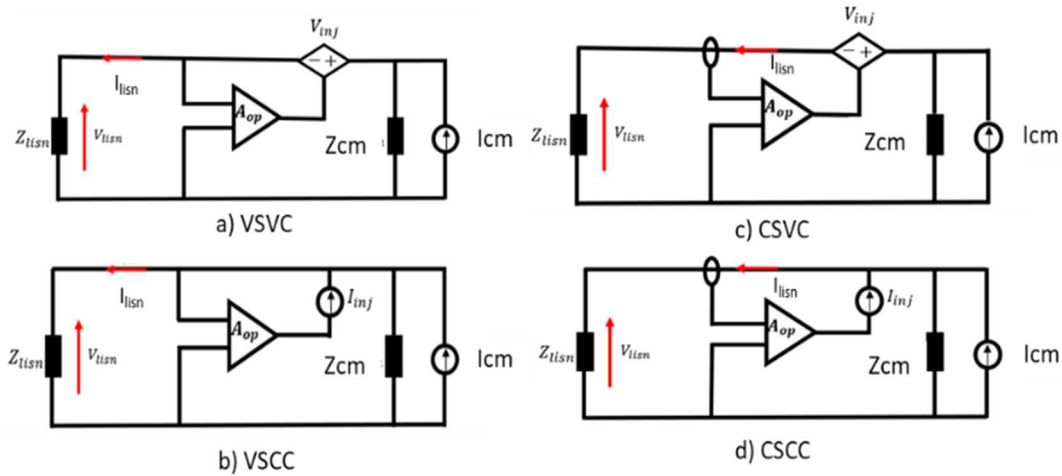


Fig. 1: Four active filter topologies. (a) Voltage sensing-voltage cancellation (VSVC). (b) Voltage sensing-current cancellation (VSCC). (c) Current sensing-voltage cancellation (CSVC). (d) Current sensing-current cancellation (CSCC)

II. VSCC AEF Analysis and modeling

The equivalent circuit model of the feedback VSCC common mode AEF is depicted in Fig. 1b. The basic principle of the AEF can be illustrated by (1), which is simply derived from Kirchoff laws. Considering that in the frequency range of interest (150 kHz – 30 MHz), the common mode impedance, Z_{cm} , is greater than the impedance of the noise receiver, Z_{lisn} , the Line Impedance Stabilization Network (LISN) current I_{lisn} is given by equation (1) where A_{op} is the absolute closed loop transfer function of the Op Amp.

$$I_{lisn} = \frac{1}{1 + Z_{lisn}A_{op}} I_{cm} \quad (1)$$

From equation (1), it is obvious that, ideally, an infinite gain of the transfer function A_{op} allows completely rejecting the noise. However, this equation does not reflect the real behavior of AEF because it does not take into account the sensing and injection transfer functions. Fig. 2a. Shows the proposed common mode AEF connected between the LISN and the converter's input. Common mode noises are sensing by a high pass RC circuit (resistor R_{sen} and two capacitors $C_{sen}/2$) and injecting through R_{inj} in series with two capacitors $C_{inj}/2$.

The operation of the AEF at the two power lines is symmetric, so the two power lines are in parallel with regard to the earth ground. An equivalent circuit model with an explicit reference is shown in Fig.2b. Based on Fig.2b, above equations can be briefly written.

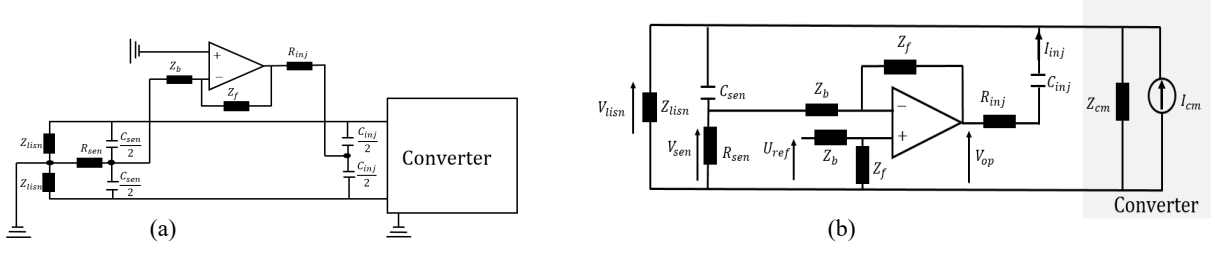


Fig.2: (a) Schematic of the proposed AEF, (b) Equivalent circuit of the proposed AEF with explicit reference

$$A_{sen} = \frac{R_{sen}}{R_{sen} + Z_{Csen}} \quad (2)$$

$$Z_{inj} = Z_{Cinj} + R_{inj} \quad A_{op} = \frac{Z_f}{Z_b} \quad (3)$$

$$A_{op} = \frac{Z_f}{Z_b} \quad (4)$$

$$V_{sen} = A_{sen} V_{lisn} \quad \text{with } R_{sen} \ll Z_b \quad (5)$$

$$I_{inj} = \frac{V_{op} - V_{lisn}}{Z_{inj}} = \frac{A_{op}(U_{ref} - A_{sen} V_{lisn}) - V_{lisn}}{Z_{inj}} \quad (6)$$

$$V_{lisn} = \frac{Z_{lisn}}{Z_{lisn} + Z_{cm}} (V_{cm} + Z_{cm} I_{inj}) \quad (7)$$

Sensing noises are compared to zero reference, $U_{ref} = 0$, (U_{ref} grounded), so expressions (5), (6) and (7) allow writing the closed loop transfer function of the system (8).

$$\frac{V_{lisn}}{I_{cm}} = \frac{\frac{Z_{cm} \cdot (Z_{lisn} // Z_{inj})}{Z_{lisn} // Z_{inj} + Z_{cm}}}{1 + \frac{Z_{lisn} // Z_{cm}}{Z_{lisn} // Z_{cm} + Z_{inj}} A_{op} A_{sen}} \quad (8)$$

A_{op} is the absolute closed loop transfer function gain of the inverting operational amplifier, and A_{sen} is the sensing transfer function. From equation (8), an infinite gain of A_{op} allows completely rejecting EMI noise ($V_{lisn} \approx 0$).

A. Feedback Loop Gain and attenuation of VSCC AEF

The AEF is basically a feedback system with an analog-input and an analog-output, and its stability should be carefully designed and guaranteed. If the system is unstable, the system can oscillate even when the converter is not supply and common mode noise can be amplified. The stability study is done with the open loop gain transfer function, T_o , which can be obtained from the closed loop transfer function. Assuming that $Z_{cm} \gg Z_{lisn}$ in the interest frequency range, the open loop gain, T_o , is given by equation (9)

$$T_o = \frac{Z_{lisn} // Z_{cm}}{Z_{lisn} // Z_{cm} + Z_{inj}} A_{op} A_{sen} = \frac{Z_{lisn}}{Z_{lisn} + Z_{inj}} A_{op} A_{sen} \quad (9)$$

From equation (9), we can see that if the condition $Z_{cm} \gg Z_{lisn}$ is satisfied, stability and design of AEF is independent of common mode noise source contrary to the passive filter that the knowledge of the common mode noise is essential for design. Moreover, the performance of an EMI filter is quantified by its attenuation, which is its ability to mitigate interferences. The attenuation is defined as the ratio of

the voltage across Z_{lisn} without the active filter to that with the active filter. The voltage across Z_{lisn} with the active filter is obtained from equation (8) and that without filter is given by equation (10).

$$V_{lisn,wo\ filter} = \frac{Z_{lisn} Z_{cm}}{Z_{lisn} + Z_{lisn}} I_{cm} \quad (10)$$

Then, the attenuation of VSCC AEF is rewritten as

$$A_{tt} = \frac{V_{lisn,wo\ filter}}{I_{cm}} \frac{I_{cm}}{V_{lisn,with\ filter}} = (1 + T_o) \left(1 + \frac{Z_{lisn}}{Z_{inj}} \right) \quad (11)$$

From equation (11), we can conclude that the attenuation is proportional to the feedback loop gain T_o . Therefore in the design of the VSCC active filter, a compromise between stability and high attenuation is necessary because both depend on T_o . Substituting equations (9) in (11), the attenuation can be rewrite as equation (12)

$$A_{tt} = (1 + T_o) \left(1 + \frac{Z_{lisn}}{Z_{inj}} \right) = 1 + \frac{Z_{lisn}}{Z_{inj}} (1 + A_{sen} A_{op}) \quad (12)$$

From equation (12), a typical model of the LISN is necessary to calculate the impedance Z_{lisn} . The LISN used is the DO160 ComPower LI-325. An external 10uF capacitor is necessary in power port side to satisfy the requirement specified in the DO160 standard. The impedance between the LISN converter port and ground is measured with the external 10uf capacitor connected.

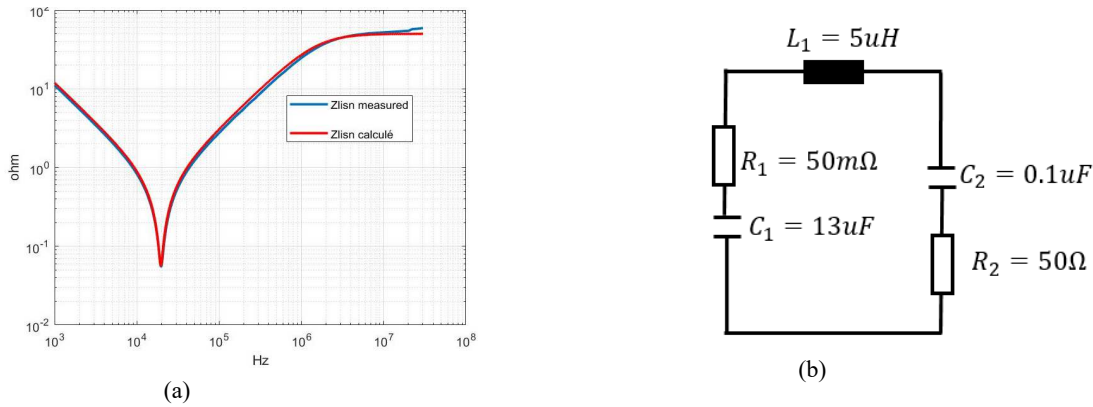


Fig 3: (a) Comparison of the impedance Li-325 DO160 LISN calculated and measured, (b) Circuit model of LISN

Fig.3a shows the impedance of LISN measured and modeled. We can see that the model matches well with the measurement. The circuit model is depicted in Fig.3b where the external 10uF capacitor is taking into account in the capacitor C_1 . However, in common mode model, there are two LISN in parallel, which can be modeled as a single equivalent impedance. Also within the concerned 'RF' frequency range, the impedances of the two capacitors 13uF and 0.1uF can be ignored, so the equivalent CM impedance of LISN can be approximately modeled as an inductance of 2.5uH in parallel with a resistance of 25Ω as depicted in Fig.3c.

$$Z_{lisn} = \frac{sL_{lisn}R_{lisn}}{sL_{lisn} + R_{lisn}} \quad \text{with } L_{lisn} = 2.5\mu H \text{ and } R_{lisn} = 25\Omega \quad (13)$$

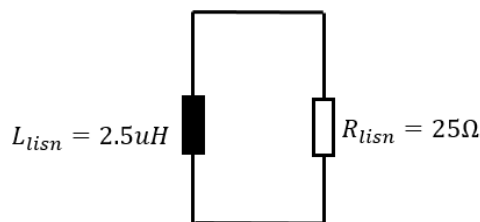


Fig 3c: Equivalent common mode impedance of LISN ignoring capacitors

Substituting equations (2), (3) and (13) in (12) allow to rewrite

$$A_{tt} = 1 + \frac{sL_{lisen}R_{lisen}}{sL_{lisen} + R_{lisen}} \frac{sC_{inj}}{1 + sR_{inj}C_{inj}} \left(1 + \frac{sR_{sen}C_{sen}}{1 + sR_{sen}C_{sen}} A_{op} \right) \quad (14)$$

B. Design guidelines of the proposed VSCC common mode AEF

In this section, the practical design guidelines for the proposed VSCC common mode AEF are developed with consideration of performance and stability.

a) operating frequency range and maximum attenuation

The first step of the design an EMI filter is to determine the required attenuation and the operation frequency range of filter. This approach remains valid in the case of AEF. Keep in mind that a high closed loop gain of the inverting amplifier is necessary to reject EMI noise. From equation (14), the closed loop transfer function A_{op} can provide the necessary closed loop gain and compensates the pole of the detection circuit ($R_{sen}C_{sen}$). Assuming the amplifier gain is designed to be equation (15) with ω_k is the cutoff frequency at which the **closed loop gain** of opamp start to roll off which can be found in the datasheet of the operational amplifier. The attenuation becomes independent of the sensing circuit.

$$A_{op} = \left| -\frac{1 + sR_fC_f}{sR_bC_f \left(1 + \frac{s}{\omega_k} \right)} \right| = \frac{1 + sR_fC_f}{sR_bC_f \left(1 + \frac{s}{\omega_k} \right)} \quad \text{with } R_fC_f = R_{sen}C_{sen} \quad (15)$$

Then, the attenuation becomes

$$A_{tt} = 1 + \frac{sL_{lisen}R_{lisen}}{sL_{lisen} + R_{lisen}} \frac{sC_{inj}}{1 + sR_{inj}C_{inj}} \left(1 + \frac{R_f}{R_b \left(1 + \frac{s}{\omega_k} \right)} \right) \quad (16)$$

For convenience, the minimum operation frequency, f_{min} , is proposed as the lowest frequency boundary that the attenuation is positive and its can be found from the low frequency model approximation of equation (16). In low frequency ω_k can be ignored and equation (16) becomes equation (17).

$$A_{tt} = \frac{s^2 + 2m\omega_n \cdot s + \omega_n^2}{\omega_n^2} \frac{1}{\left(1 + s \frac{L_{lisen}}{R_{lisen}} \right) (1 + sR_{inj}C_{inj})} \quad (17)$$

With

$$\omega_n = \sqrt{\frac{R_{lisen}}{L_{lisen}C_{inj} \left[R_{inj} + R_{lisen} \left(1 + \frac{R_f}{R_b} \right) \right]}} \quad \text{and} \quad m = \frac{L_{lisen} + R_{lisen}R_{inj}C_{inj}}{2\omega_n}$$

The minimum operation frequency is obtained as

$$f_{min} = \frac{\omega_n}{2\pi} = \frac{1}{2\pi} \sqrt{\frac{R_{lisen}}{L_{lisen}C_{inj} \left[R_{inj} + R_{lisen} \left(1 + \frac{R_f}{R_b} \right) \right]}} \quad (18)$$

To obtain the full operating frequency range of the AEF, the high frequencies boundary and final value must be determined. They are obtained from the high frequency approximation of equation (16). In high frequency, the feedback capacitor of inverting amplifier can be ignored (the zero of inverting opamp transfer function is in low frequency). On other hands, the impedances of the LISN and injection circuits

are respectively equal to R_{lism} and R_{inj} . Therefore, the maximum operating frequency and the high frequency final value can be determined based on the high frequency approximation of the attenuation given by equation (19)

$$A_{tt} = \left[1 + \frac{R_{lism}}{R_{inj}} \left(1 + \frac{R_f}{R_b} \right) \right] \frac{1 + \frac{s}{\omega'_k}}{1 + \frac{s}{\omega_k}} ; \text{ with } \omega'_k = \frac{1 + \frac{R_{lism}}{R_{inj}}}{\omega_k \left[1 + \frac{R_{lism}}{R_{inj}} \left(1 + \frac{R_f}{R_b} \right) \right]} \quad (19)$$

The maximum operation frequency and final value are obtained as

$$f_{max} = \frac{\omega_k}{2\pi} = \quad \text{and} \quad A_{tt,HF} = 1 + \frac{R_{lism}}{R_{inj}} \quad (20)$$

Now, an interesting asymptotic behavior of attenuation can be extracted and illustrated in Fig.4. The necessary frequencies boundaries and gain are determined.

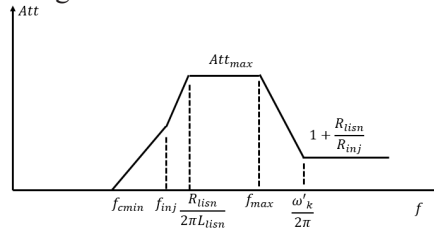


Fig 4: Ideal asymptotic behavior of attenuation

b) Sensing circuit

The sensing circuit is a high pass RC circuit composed of a sensing capacitor C_{sen} and resistor R_{sen} . From equation (16), after pole compensation, attenuation is independent from the sensing parameters but the open loop gain of the AEF depends. Therefore, the detection circuit can be used to sensing noise and avoid stability issue in low frequency without affecting attenuation. By fixing a sensing frequency close to the switching frequency and choosing R_{sen} according to equation (5), the sensing capacitor is given by equation (21).

$$C_{sen} = \frac{1}{2\pi f_{sen} R_{sen}} \quad (21)$$

c) Amplifier circuit

The minimum amplification gain, R_f/R_b , required to achieve the necessary attenuation is obtained from equation (16) and it is given by (22)

$$\left. \frac{R_f}{R_b} \right|_{dB} = A_{tt,dB} + \left| \frac{Z_{inj} \left(1 + \frac{s}{\omega_k} \right)}{Z_{lism}} \right|_{dB} \quad (22)$$

Moreover, the operational amplifier is the central element of the VSCC common mode AEF. The choice of this active device is important since its limitations will greatly affect the performances of the AEF. It must be high speed and operate in linear mode and its current capacity should be sufficient to avoid saturation. A push-pull current amplification can be used if the Op-amp has a low output current. In addition, it should have a high frequency bandwidth ($GBP \geq 30\text{MHz}$).

d) Injection circuit

The minimum operating frequency f_{min} depends on the cut-off frequency of the injection circuit. By fixing a lowest boundary frequency f_{min} of the operation frequency range of the filter, and choosing an injection resistor R_{inj} , the injection capacitor is determined based on equation (23). Keep in mind that

a high injection resistor decreases the maximum attenuation of filter and a lowest value cannot be chosen due to the stability and capability of opamp to drive a capacitive load (injection capacitor).

$$C_{inj} = \frac{R_{lism}}{L_{lism} \left[R_{inj} + R_{lism} \left(1 + \frac{R_f}{R_b} \right) \right] (2\pi f_{min})^2} \quad (23)$$

II. Implementation and validation

To verify the validity of the proposed methodology, the test setup is established on 14V/42V – 27W Boost operating at 115 kHz switching frequency. The transfer functions previously calculated are validate in both simulations and measurements. The performance of the proposed AEF is then by spectrum analyzer measurements.

a) Common mode current measurement without filter

The common mode current spectrum are measured and compared to the DO160 standard to determine the operating frequency range and the required maximum attenuation. Fig. 5a and 5b depict the experimental temporal and spectrum common mode noise without filter.

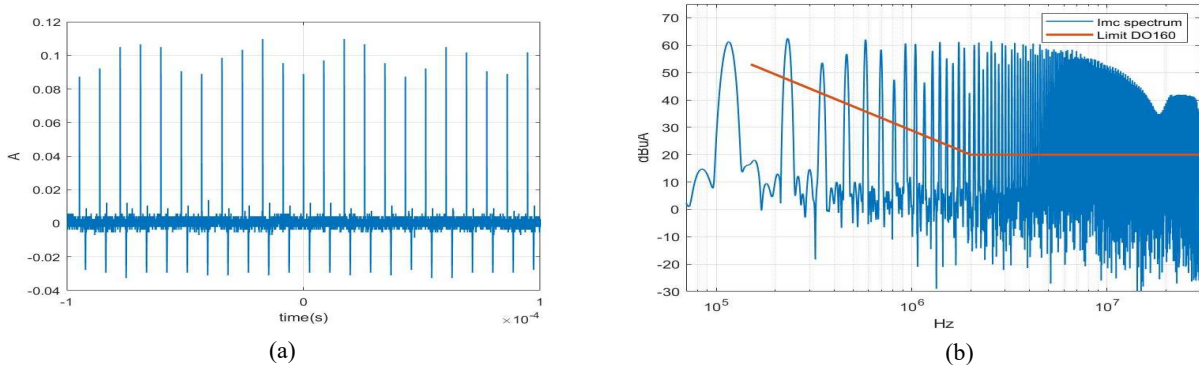


Fig 5 (a) Temporal common mode noise current without filter, (b) Spectrum of common mode noise without filter

Based on Fig. 5b, a common mode EMI Filter is necessary over the entire ‘RF’ frequency range. To satisfy the standard in low frequency, an active filtering is proposed in the frequency range below 1MHz. Above 1MHz, a passive filter can be used to achieve the required attenuation and satisfy the DO160 standard. To determine the required minimum amplification, the maximum attenuation in the active filter operating frequency range is determined by subtract the 8th harmonic to the DO160 limit.

$$A_{ttmax} = I_{mc} - Limit(DO160) = 60dB\mu A - 30dB\mu A = 30$$

As we want to improve the effectiveness of AEF in low frequency, the lowest and highest operating frequency of AEF are respectively fixed at $f_{cmin} = 30$ kHz and $f_{cmax} = 1$ MHz. Even if the switching frequency is at 115kHz, the minimum frequency boundary is chosen too low in case it needs to use this AEF for application where the switching frequency would be lower. Moreover, as the injection amplifier supply the injection current, for an ideal filter $I_{inj} = I_{cm}$. Therefore, the output current of opamp must be at least equal to I_{mc} . Based on Fig. 5a, the minimum output current capability of the opamp is 120 mA.

b) Sensing , injection and amplifier circuits and stability

The injection resistor should not be high to reduce the maximum attenuation but also a reasonable value must be chosen to assure stability of opamp driving capacitive load. So a value of 6.8Ω is chosen. Then the injection capacitor is determined based on (23) and equal to $0.2\mu F$. The minimum required amplification to achieve the required attenuation is calculated from (22) and shown in Fig.6a.

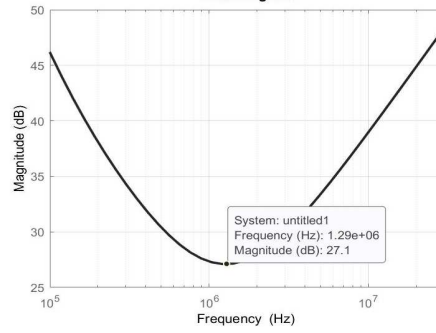


Fig 6a: Minimum required amplification

Based on Fig.6a, to achieve an attenuation of 30dB at 1MHz, a minimum amplification of 27dB is required. Moreover, Opamps are generally of two types: voltage feedback opamp (VFA) and current feedback opamp (CFA). For a VFA, its gain-bandwidth product is constant, so the gain is inversely proportional to the bandwidth. On other hands, CFA has a bandwidth independent of its gain, so it can achieve a wider bandwidth than VFA. So a CFA is chosen in this application. Due to the high common mode current, a Texas Instrument CFA, THS3121, has been selected. It exhibits a 475mA output current capability as well as a large bandwidth of xxxMHz.

The attenuation is independent of the sensing parameters but the open loop gain of the AEF depends. From (16) the pole of detection must be compensated by the zero of the CFA. So, Sensing frequency can be chosen close to switching frequency 115kHz, and it is fixing at 70kHz and sensing resistor is equal to 110Ω, the component values are given in Table 1.

Table 1: Component Value

Component	Value
R_f	33kΩ
C_f	68pF
R_b	1 kΩ
R_{sen}	110
C_{sen}	2 x 10nF
R_{inj}	6.8 Ω
C_{inj}	2x0.1uF
CFA	THS3121

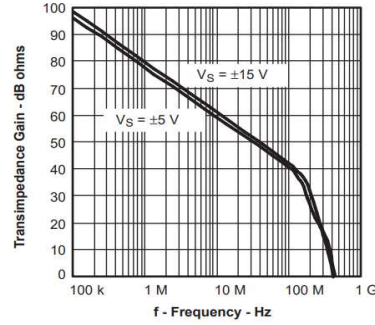


Fig 6b: Transimpedance of THS3121

The open loop transimpedance gain Z of THS3121 is given by Fig.6b. In frequency below 30MHz it can be expressed as

$$Z = \frac{Z_{dc}}{1 + \frac{s}{\omega_p}} \quad \text{with } \omega_p = 2\pi(100\text{kHz}) \quad (24)$$

Z_{dc} is the DC transimpedance. As the transimpedance at the cutoff frequency $f_p = 100\text{kHz}$ is equal to 100dB then it can conclude that $Z_{dc} = 103\text{dB}$. For a CFA, the absolute closed loop gain of an inverting opamp is expressed as

$$A_{op} = \frac{\frac{Z_f}{Z_b}}{1 + \frac{Z_f}{Z}} \approx \frac{Z_{dc}}{R_b} \frac{1 + sR_fC_f}{\left(1 + \frac{s}{\omega_1}\right)\left(1 + \frac{s}{\omega_k}\right)} \quad (25)$$

Where ω_1 is a very low frequency pole, which approximatively located at $(R_f + Z_{dc})C_f$ and ω_k is the high frequency closed loop gain pole, which define the closed loop bandwidth of the opamp. As the DC transimpedance Z_{dc} is very high, we fund again the equation (15) from equation (25) of the absolute closed loop in our frequency range by taking the behavior beyond ω_1 . Based on Fig.7b, the calculated

expression of A_{op} matches well with measurement. As mentioned before, the stability should be carefully designed and guaranteed to avoid oscillation or damage the filter.

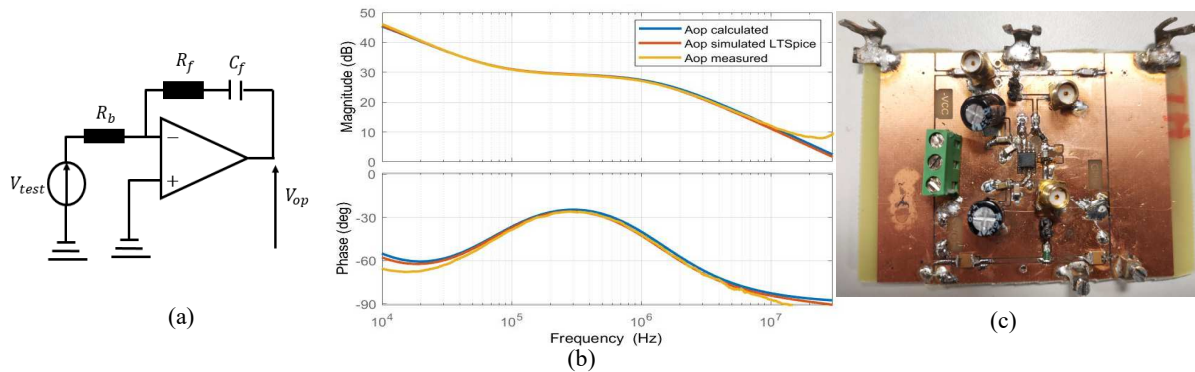


Fig 7. (a) Absolute Transfer function $A_{op} = Z_f/Z_b$ measurement, (b) Comparison between A_{op} calculated, simulated and measured, (c) Proposed common mode AEF

Experimentally, to measure the loop gain from the circuit model, the feedback loop is disconnected at the opamp input and a test voltage is applied in the input of the amplifier from the disconnected node, while the converter is not supplied based on Fig.8a

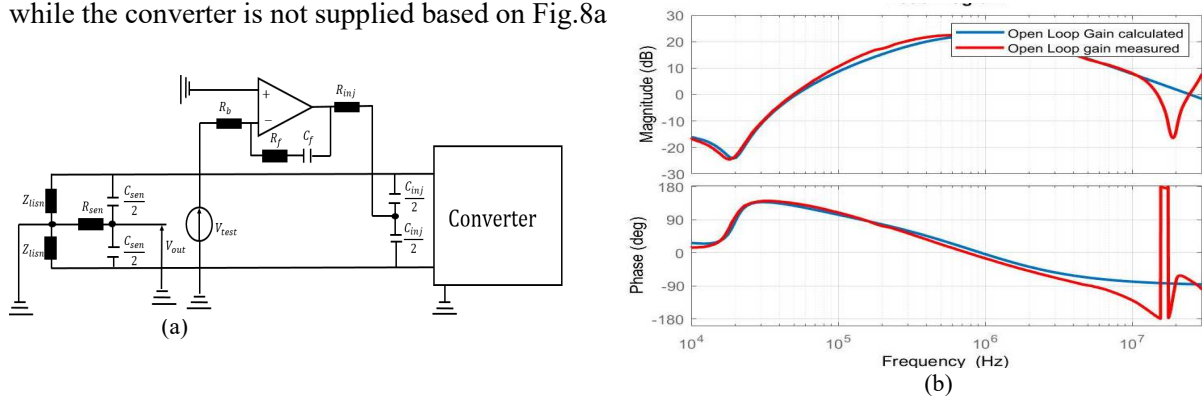


Fig.8 (a) Open loop gain measurement $T_o = -V_{out}/V_{test}$, (b) Comparison between calculated and measured open loop gain transfer function

Based on Fig.8b, the loop transfer function, T_o , measured and calculated match. There is a slight difference in high frequency above 10MHz, where a resonance due to common mode impedance occurs. The loop transfer function crosses unity gain both when the loop gain is rising and falling. For such a system, the closed loop system is stable if the open loop transfer function has an amplitude less than unity at all frequencies corresponding to the phase equal to $-180 - nx360$, where $n = 0, 1, \dots \infty$. Based on Fig.8b, the stability criteria mentioned above is satisfied in low frequency contrary to high frequency around 15MHz.

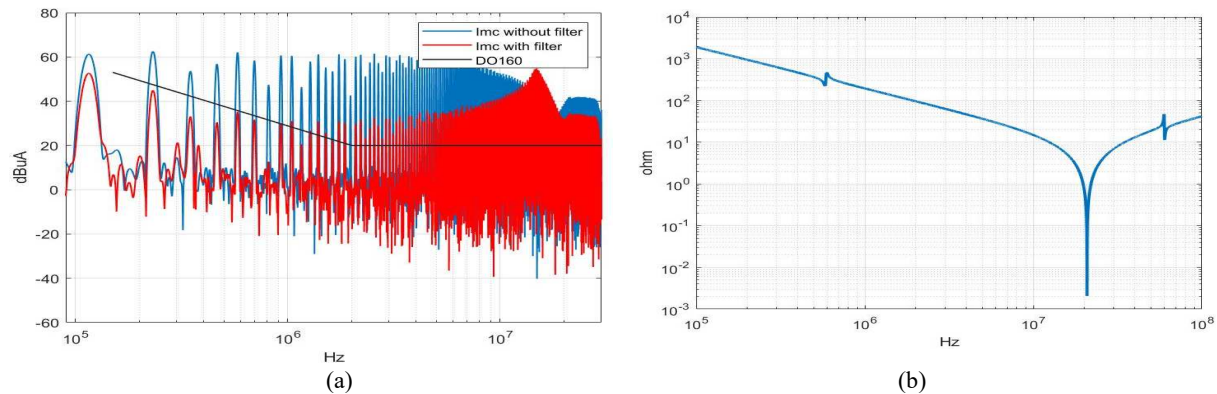


Fig 9: (a) Comparison between common mode noise spectrum with and without AEF, (b) Common mode impedance

Based on Fig.9a, in the operating frequency range of the AEF, the standard is met. An attenuation of 10dB is reached at 115kHz. Above the high frequency boundary of the AEF, 1MHz, a passive filter can

be used to reach the standard in whole the ‘RF’ frequency range. On the other hand, the high frequency instability results an amplification of common mode noise around 15MHz. This frequency of 15MHz is higher than the operating frequency range of the AEF, a small passive filter can be used to attenuate the noise amplification. To understand well the origin of the resonance at 15MHz, the common mode impedance is measured and shown in Fig.9b. It is not capacitive in the whole ‘RF’ frequency range and the assumption $Z_{lisen} // Z_{cm}$ equal Z_{lisen} is not valid.

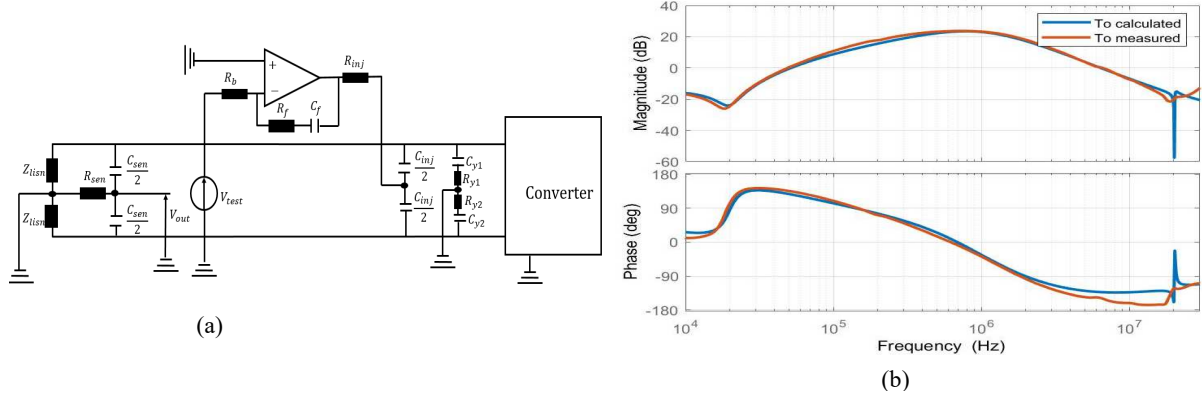


Fig.10 (a) Open loop gain measurement with Cy, (b) Comparison between calculated and measured open loop gain transfer function with Cy

To limit the effect of common mode noise, two capacitors Cy of 4.7nF in series with 1Ω have been used based on fig.10(a). So, the expression of open loop gain (9) becomes (26) and no resonance appears in high frequency as shown in Fig.10b. The stability criteria is satisfied and noises are not amplified as shown in Fig.11b.

$$T_o = \frac{Z_{lisen} // (Z_{cm} // Z_{cy})}{Z_{lisen} // (Z_{cm} // Z_{cy}) + Z_{inj}} A_{op} A_{sen} \quad (26)$$

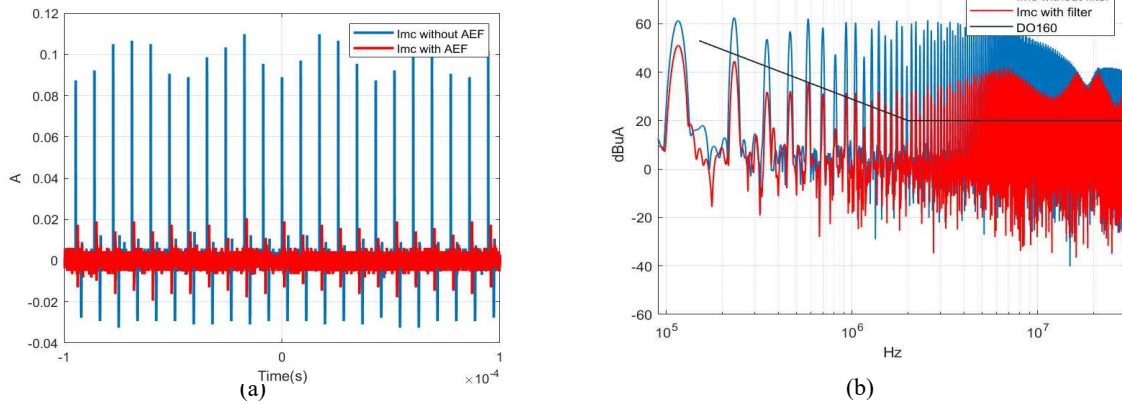


Fig 11a: Comparison between Imc with filter and without filter, (b) Comparison between common mode noise spectrum with and without filter

III. Conclusion

In this paper, the study and design of a VSCC AEF were discussed. A design guideline has been established and validated by simulation and experimental measurements. Stability has been checked and the effect of parasitic inductance of common mode impedance has shown. Based on the design guideline components value are calculated and we can see that the DO160 standard was met up to 1MHz. The filter still attenuated above 1 MHz but not sufficiently to comply with the standard. Therefore a passive filter could be added to comply the standard over frequency range [115kHz – 30MHz]. This study also shows us the role of active filter in hybrid filtering. In fact, active filter essentially aims to attenuate low frequencies and allow the size of the passive filter to be reduced, which would complete the filtering for very high frequencies. An attenuation of 10dB is obtained at 115kHz

IV. REFERENCE

- [1] X. Pei, J. Xiong, and J. Chen, “Analysis and Suppression of Conducted EMI Emission in PWM inverter,” p. 6.
- [2] T. Ninomiya, M. Shoyama, C.-F. Jin, and G. Li “EMI ISSUES IN SWITCHING POWER CONVERTERS,” p. 6.
- [3] M. Ali, E. Laboure, and F. Costa, “Integrated Active Filter for Differential-Mode Noise Suppression,” *IEEE Trans. Power Electron.*, vol. 29, no. 3, pp. 1053–1057, Mar. 2014
- [4] J. Biela, A. Wirthmueller, R. Woespe, M. L. Heldwein, K. Raggl, and J. W. Kolar, “Passive And Active Hybrid Integrated EMI Filters,” *IEEE Trans. Power Electron.*, vol. 24, no. 5, pp. 1340–1349, May 2009
- [5] M. Pasko and M. Szymczak, “Analysis and simulation of the basic structures of active EMI filters,” p. 14.
- [6] W. Chen, W. Zhang, X. Yang, Z. Sheng, Z. Wang, “An Experimental Study of Common-and Differential-Mode Active EMI Filter Compensation Characteristics,” *IEEE Trans on Electromagnetic Compatibility*, vol. 51, no. 3, p. 9, 2009